Dispersion profiles of the absorptive response of a two-level system interacting with two intense fields

H. Friedmann and A. D. Wilson-Gordon
Department of Chemistry, Bar-Ilan University, Ramat Gan 52100, Israel
(Received 15 October 1986; revised manuscript received 13 January 1987)

When a two-level system interacts resonantly with a saturating pump laser, the absorption profile of a probe wave in the Rabi sidebands resembles two separate dispersion profiles. At sufficiently high probe intensity this effect is accompanied by a dispersive profile in the pump-wave absorption, considered as a function of the probe-wave frequency, and also by a dip in the population of the upper state of the two-level system. The relative stabilization of the ground state is interpreted in terms of two-laser-photon processes where absorption of a pump (probe) photon is followed by stimulated emission of a probe (pump) photon. The dispersive absorption profile is attributed to the competition between three- and four-photon scattering processes.

I. INTRODUCTION

A three-peaked resonance fluorescence spectrum has been predicted by Mollow[1] when a two-level system interacts resonantly ($\omega_1=\omega_{ba}$) with a saturating pump laser. This behavior has been observed in both the collisionless[2] and collisional[3] regimes. The behavior of a weak probe-wave absorption profile in the presence of a pump wave tuned directly to the resonance frequency has also been studied theoretically by Mollow[4] and experimentally in an atomic beam by Wu *et al.*[5] Here again a three-peaked spectrum is obtained reminiscent of the two-level system resonance fluorescence spectrum. However, the two sideband absorption peaks whose detuning $|\Delta_2|=|\omega_{ba}-\omega_2|$ from the resonance frequency ω_{ba} is slightly larger than the pump Rabi frequency $2|V_1|=|\mu_{ba}E_1|/\hbar$ are part of the dispersionlike features whose negative absorption (gain) peaks appear on that side of the Rabi frequency which is closer to the resonance frequency (see Fig. 1). Note that in the qualitative discussion of the physical effects, we assume, unless otherwise stated, that $2|V_1|\gg(1/T_2)$ so that the role of relaxation is limited to attaining the steady-state regime.

No intuitive explanation for the appearance of the dispersionlike features has been offered so far. In order to gain some insight into this problem we have generalized the approach of Mollow to the case where the pump and probe lasers are of arbitrary strength. These calculations are similar to those carried out by Toptygina and Fradkin[6] and by Agarwal and Nayak[7] for different purposes. Experimental results for pump and probe absorptions in strong bichromatic fields are also available.[8] Interaction with a strong probe will of course alter the response of the system to pump radiation. We find in general that whenever the probe absorption increases, the pump absorption decreases and vice versa. Thus the dispersive features of the probe absorption line shape are also obtained in the pump spectrum but with opposite tendencies (see Fig. 2). This effect has not so far been demonstrated in the literature.

A theoretical analysis, presented in Sec. III, of the probe-absorption spectrum in the limit of weak-probe intensity and zero pump-laser detuning ($\Delta_1=\omega_{ba}-\omega_1=0$) indicates that the dispersive line shape arises from the competition of a three-photon scattering (TPS) process, involving the absorption of one pump photon and one probe photon, and a four-photon scattering (FPS) process,

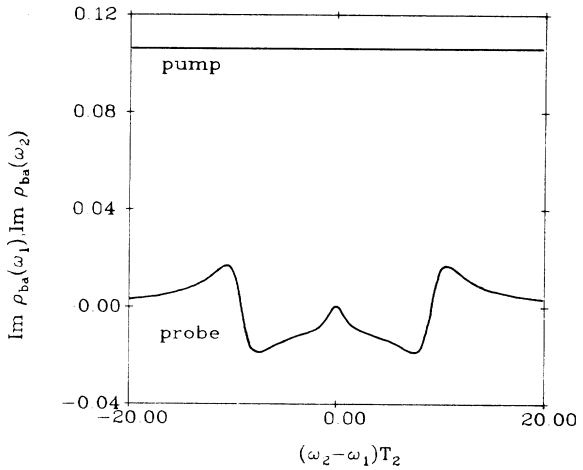

FIG. 1. Weak-probe absorption spectrum in the presence of strong resonant pump absorption. When the pump laser frequency ω_1 equals the two-level resonance frequency ω_{ba}, the weak-probe-absorption profile calculated to lowest order in the probe-laser field E_2 exhibits two dispersion profiles centered at the Rabi sideband frequencies: $\omega_2-\omega_1\simeq\pm 2|V_1|$, where ω_2 is the probe-laser frequency and $2|V_1|$ the pump Rabi frequency $|\mu_{ab}E_1|/\hbar$. To first order in the weak-probe field strength E_2, the pump-absorption profile represented by $\mathrm{Im}\rho_{ba}(\omega_1)$ is independent of the weak-probe frequency. Note the broad region of probe amplification in the probe-frequency region $-2|V_1|\lesssim\omega_2-\omega_1\lesssim|2V_1|$. Parameters used are $|V_1|T_2=4.6$, $|V_2|T_2=10^{-5}$, $T_1=0.5T_2$, where T_2 is the transverse relaxation time and $\mathrm{Im}\rho_{ba}(\omega_2)$ is multiplied by 10^5.

involving the absorption of two pump photons and the stimulated emission of one probe photon. Both processes also involve a scattered photon. Whereas the TPS process (implying probe absorption) prevails over the higher-order nonlinear FPS process when $|\Delta_2| = |\omega_2-\omega_1| > 2|V_1|$, the opposite is true when $|\Delta_2| < 2|V_1|$ since then FPS (implying stimulated probe emission), in contrast to TPS and one-photon absorption, becomes an almost resonant process. Thus FPS may prevail over both TPS and one-photon probe absorption thereby leading to probe amplification. This amplification is obtained in the absence of population inversion and results from the irreversible nature of the FPS process.

When $|\Delta_2| \simeq 2|V_1|$, we expect that two-laser-photon processes will occur where either a probe photon is absorbed and a pump photon is emitted or a pump photon is absorbed and a probe photon emitted. The combined effect of both processes leads to no net absorption or emission of probe photons but, at moderate probe intensity, to the stabilization of the ground state and therefore to a dip in the population difference, as shown in Fig. 3. These population dips have not been pointed out before for two-level systems.

At moderate probe intensity, the decrease of resonant pump absorption with decreasing probe detuning $|\Delta_2|$ when $|\Delta_2| > 2|V_1|$ results from an increase in (mostly

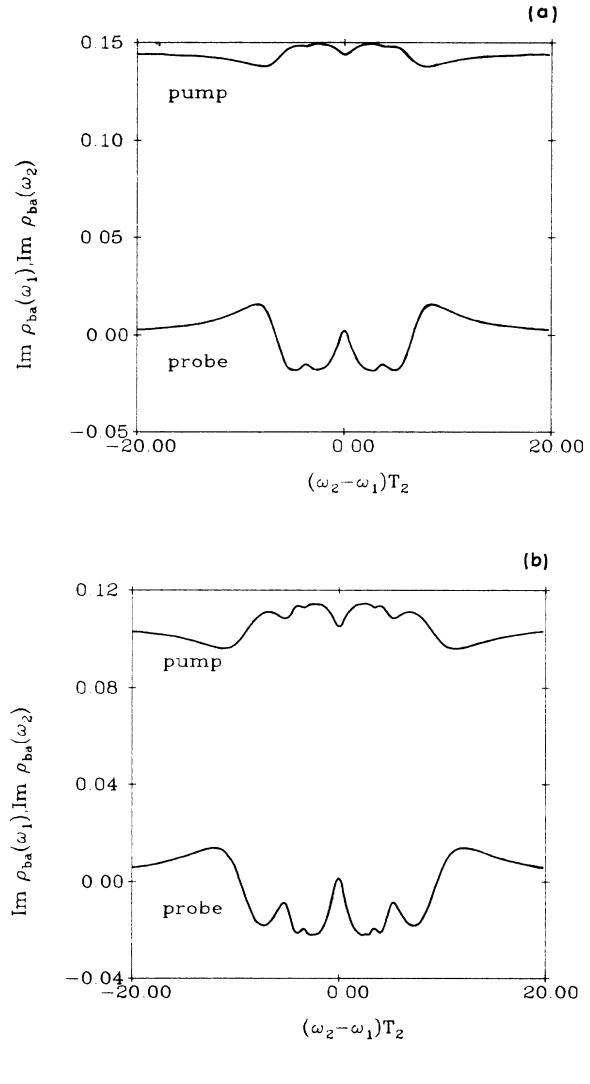

FIG. 2. Probe- and pump-absorption spectrum for strong-pump and moderate-probe intensities. At moderate probe intensities, the dispersive probe-absorption profiles are accompanied by dispersive pump-absorption profiles with opposite tendencies. As in Fig. 1, $\omega_1=\omega_{ba}$, $T_1=0.5T_2$. In (a), $|V_1|T_2=3.3$, $|V_2|T_2=1.0$, and in (b), $|V_1|T_2=4.6$, $|V_2|T_2=2.0$. The dispersion profiles are distorted and "Rabi subharmonic" peaks or dips appear in the region $-2|V_1| \lesssim \omega_2-\omega_1 \lesssim |2V_1|$.

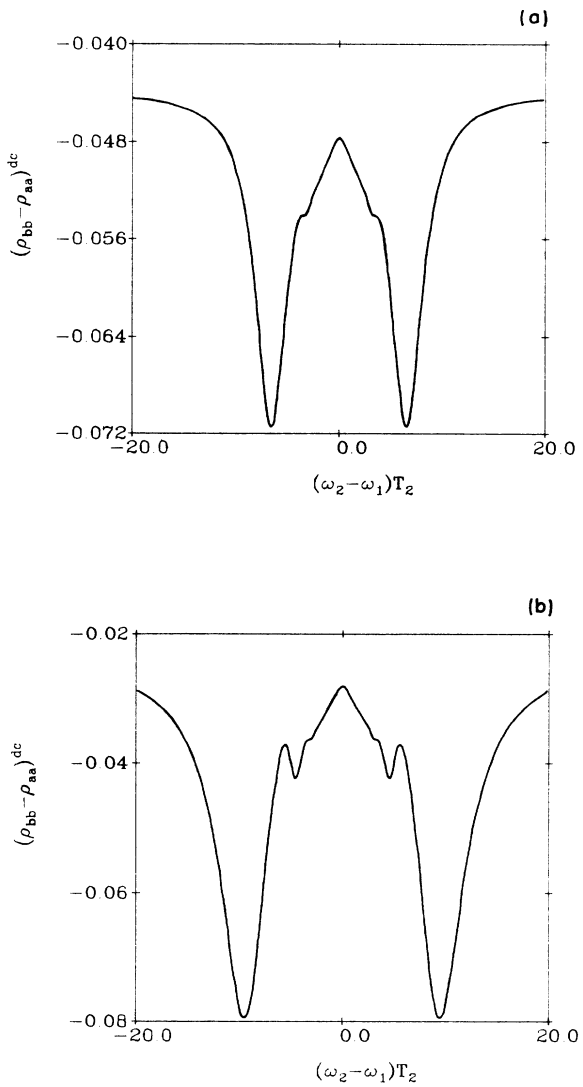

FIG. 3. Plot of d_0 which gives the long-time averaged population inversion at all points except $\omega_2=\omega_1$ [see Eqs. (17) and (18)] as a function of probe frequency for moderate probe fields. Population dips, indicative of relative ground-state stabilization, appear at the Rabi sideband frequencies. The parameters in (a) and (b) are the same as in Figs. 2(a) and 2(b), respectively.

one-photon) probe absorption and hence increased saturation of the two-level system. Another cause of the decrease in resonant pump absorption is that the probe laser shifts the two-level system out of resonance with the pump-laser frequency. When $|\Delta_2|<2|V_1|$, the FPS where two pump photons are absorbed becomes important, leading to increased absorption of the pump laser.

It should be noted that intense probe fields broaden and distort the wings of the dispersionlike absorption line shapes and a number of peaks or dips appear in the wing which is closer to the resonance frequency. As can be seen by comparing Figs. 2(a) and 2(b), the number of peaks or dips increases with the probe intensity. These additional features are not characterized by a dispersive line shape but consist of peaks or dips superimposed on the distorted dispersionlike profile discussed above. These features also have opposite behavior in the probe and pump spectra: maxima in probe absorption correspond to minima in pump absorption. They appear at detunings from the resonance which are fractions of the Rabi frequency and have been called Rabi subharmonics.[7] They are due to processes involving more than one probe-laser photon.[7–9] The three-photon processes responsible for the two small peaks in the probe spectrum and the corresponding two dips in the pump spectrum of Fig. 2(a) will be described in Sec. III (see Fig. 11).

From a practical point of view, it may be worth noting that the present study points to the possibility of obtaining tunable amplification of probe radiation (and perhaps chirping) by varying the pump Rabi frequency. On the other hand, when the probe frequency is kept constant, variation of the pump intensity will cause switching of the probe radiation from absorption to stimulated emission when the pump Rabi frequency is varied through the probe frequency (Fig. 4).

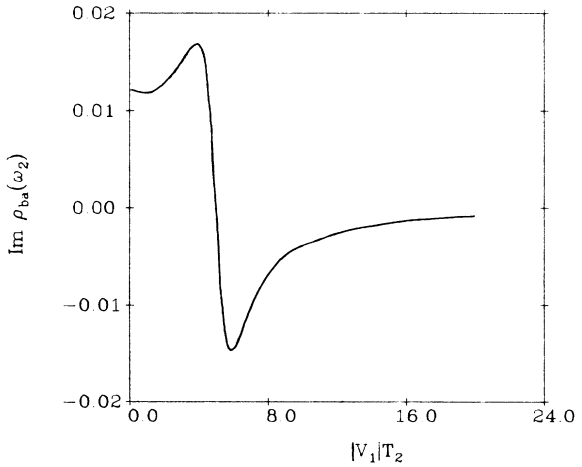

FIG. 4. Optical switching of probe absorption by varying pump intensity. The response of a two-level system to a probe detuned from resonance switches from probe absorption to probe amplification when the pump Rabi frequency $2|V_1|$ is swept through the probe detuning $|\Delta_2|=|\omega_{ba}-\omega_2|$. The parameters used in the figure are $\Delta_1=\omega_{ba}-\omega_1=0$, $\Delta_2 T_2=(\omega_{ba}-\omega_2)T_2=-10$, and $|V_2|T_2=1$.

II. BLOCH EQUATIONS

Consider the two-level system of Fig. 5 interacting with the bichromatic field

$$\mathbf{E}(t)=\tfrac{1}{2}\hat{\epsilon}[E_1+E_2\exp(-i\delta t)]\exp(-i\omega_1 t)+\text{c.c.}\ , \quad (1)$$

where ω_1 and $\omega_2=\omega_1+\delta$ are the frequencies of the bichromatic field and $E_{1,2}$ its field strengths. Denoting the Rabi frequencies by

$$2V_1=\mu_{ab}E_1/\hbar,\quad 2V_2=\mu_{ab}E_2/\hbar\ , \quad (2)$$

we may write the Bloch equations in the rotating-wave approximation as

$$i\dot{\rho}_{ab}=-(\omega_{ba}+i/T_2)\rho_{ab} -(V_1^*+V_2^*e^{i\delta t})e^{i\omega_1 t}(\rho_{bb}-\rho_{aa})\ , \quad (3)$$

$$i(\dot{\rho}_{bb}-\dot{\rho}_{aa})=2(V_1^*+V_2^*e^{i\delta t})e^{i\omega_1 t}\rho_{ba} -2(V_1+V_2e^{-i\delta t})e^{-i\omega_1 t}\rho_{ab} -(i/T_1)(\rho_{bb}-\rho_{aa})-i/T_1\ . \quad (4)$$

The steady-state solution for these equations can be written in the form (see Refs. 6, 7, and 10 for similar methods)

$$\rho_{ab}=\sum_n \rho_{ab}(n\delta-\omega_1)e^{-i(n\delta-\omega_1)t} \equiv \sum_n a_{-n}e^{-i(n\delta-\omega_1)t}=\sum_n a_n e^{i(n\delta+\omega_1)t}\ , \quad (5)$$

$$\rho_{ba}=\sum_n \rho_{ba}(n\delta+\omega_1)e^{-i(n\delta+\omega_1)t} \equiv \sum_n a_n^* e^{-i(n\delta+\omega_1)t}\ , \quad (6)$$

$$\rho_{bb}-\rho_{aa}=\sum_n (\rho_{bb}-\rho_{aa})^{n\delta}e^{-in\delta t} \equiv \sum_n d_{-n}e^{-in\delta t}\ . \quad (7)$$

Inserting these expressions into the Bloch equations

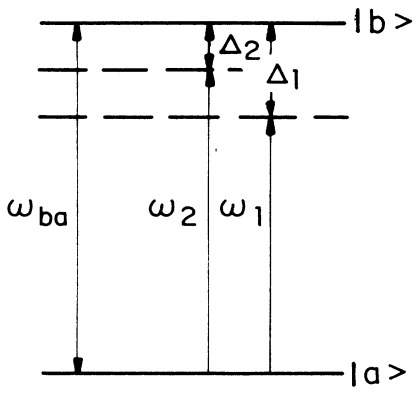

FIG. 5. Two-level system interacting with a bichromatic field.

leads to the following recursion formulas:

$$\rho_{ab}(-n\delta-\omega_1)\equiv a_n=-(\Delta_1-n\delta+i/T_2)^{-1}\times(V_1^*d_n+V_2^*d_{n-1})\ , \tag{8}$$

$$(\rho_{bb}-\rho_{aa})^{-n\delta}\equiv d_n=P_n^{-1}[(-i/T_1)\delta_{n0}+Q_nV_1V_2^*d_{n-1}+R_nV_1^*V_2d_{n+1}]\ , \tag{9}$$

where

$$P_n=-n\delta+i/T_1-4(n\delta-i/T_2)\{|V_1|^2[\Delta_1^2-(n\delta-i/T_2)^2]^{-1}+|V_2|^2[\Delta_2^2-(n\delta-i/T_2)^2]^{-1}\}\ , \tag{10}$$

$$Q_n=2[(2n-1)\delta-2i/T_2]\times[(\Delta_1-n\delta+i/T_2)(\Delta_2+n\delta-i/T_2)]^{-1}\ , \tag{11}$$

$$R_n=2[(2n+1)\delta-2i/T_2]\times[(\Delta_1+n\delta-i/T_2)(\Delta_2-n\delta+i/T_2)]^{-1}\ , \tag{12}$$

$$\Delta_1=\omega_{ba}-\omega_1,\quad \Delta_2=\omega_{ba}-\omega_2,\quad \delta=\omega_2-\omega_1\ . \tag{13}$$

Since $\rho_{bb}-\rho_{aa}$ is real, we note that

$$d_{-n}=d_n^*,\quad d_0=d_0^*\ . \tag{14}$$

The Fourier components $\rho_{ab}(n\delta-\omega_1)\equiv a_{-n}$, $\rho_{ba}(n\delta+\omega_1)=\rho_{ab}^*(-n\delta-\omega_1)\equiv a_n^*$, and $(\rho_{bb}-\rho_{aa})^{n\delta}\equiv d_{-n}$ are related to important physical properties.[11] Thus, for example,

$$\rho_{ba}(\omega_1)=\rho_{ab}^*(-\omega_1)=a_0^*=-\left[\frac{V_1d_0+V_2d_1}{\Delta_1-i/T_2}\right] \tag{15}$$

determines the absorption and dispersion spectrum of the pump laser,

$$\rho_{ba}(\omega_2)=\rho_{ab}^*(-\omega_2)=a_1^*=-\left[\frac{V_2d_0+V_1d_1}{\Delta_2-i/T_2}\right] \tag{16}$$

determines the same properties for the probe laser, and

$$(\rho_{bb}-\rho_{aa})^0\equiv(\rho_{bb}-\rho_{aa})^{\rm dc}\equiv d_0 \tag{17}$$

gives the long-time average of the population inversion $\langle\rho_{bb}-\rho_{aa}\rangle_{\rm av}$ if $\delta\neq0$. When $\delta=0$,

$$\langle\rho_{bb}-\rho_{aa}\rangle_{\rm av}=\sum_n d_n \tag{18}$$

and becomes equal to the population inversion for a single field with field strength E_1+E_2 [Eq. (1)].

The intensity of the four-wave-mixing signal of frequency $\omega_4=2\omega_1-\omega_2$ is determined by the absolute value of the square of

$$\rho_{ab}(\omega_2-2\omega_1)\equiv a_{-1}=-\left[\frac{V_1^*d_1^*+V_2^*d_2^*}{\Delta_1+\delta+i/T_2}\right]\ . \tag{19}$$

In Eqs. (15)–(19) we have used Eqs. (8) and (14).

Introducing the ratio

$$Z_n\equiv d_n/d_{n-1}\ , \tag{20}$$

we write Eq. (9) in the form

$$P_n=Q_nV_1V_2^*Z_n^{-1}+R_nV_1^*V_2Z_{n+1},\quad n\neq0\ , \tag{21}$$

$$P_0d_0=-i/T_1+Q_0V_1V_2^*Z_1^*d_0+R_0V_1^*V_2Z_1d_0\ . \tag{22}$$

In the last equation we have inserted $d_{-1}=d_1^*=Z_1^*d_0$ and $d_1=Z_1d_0$ by virtue of Eqs. (14) and (20).

Eq. (21) can be written as

$$Z_n=\frac{Q_nV_1V_2^*}{P_n-R_nV_1^*V_2Z_{n+1}}\ , \tag{23}$$

which shows that Z_n can be expressed as a continued fraction:

$$Z_n=\frac{U_nV_1V_2^*}{1-\dfrac{S_n|V_1|^2|V_2|^2}{1-\cdots}},\quad U_n=\frac{Q_n}{P_n},\quad S_n=\frac{R_n}{P_n}U_{n+1}\ . \tag{24}$$

Equations (10) and (12) show that

$$R_0=-Q_0^* \tag{25}$$

allowing us to rewrite Eq. (22) in the form

$$d_0\equiv(\rho_{bb}-\rho_{aa})^{\rm dc}_{\delta\neq0}=-(i/T_1)(P_0+2i\,{\rm Im}R_0V_1^*V_2Z_1)^{-1}\ . \tag{26}$$

III. RESULTS AND DISCUSSION

The pulse and probe absorption spectra are proportional to ${\rm Im}\rho_{ba}(\omega_1)$ and ${\rm Im}\rho_{ba}(\omega_2)$.[11] From Eqs. (15), (16), (20), and (26), it follows that

$$\rho_{ba}(\omega_1)=\frac{V_1+V_2Z_1}{\Delta_1-i/T_2}\frac{i/T_1}{P_0+2i\,{\rm Im}R_0V_1^*V_2Z_1}\ , \tag{27}$$

$$\rho_{ba}(\omega_2)=\frac{V_2+V_1Z_1^*}{\Delta_2-i/T_2}\frac{i/T_1}{P_0+2i\,{\rm Im}R_0V_1^*V_2Z_1}\ , \tag{28}$$

where [see Eq. (24)]

$$Z_1=\frac{U_1V_1V_2^*}{1-\dfrac{S_1|V_1|^2|V_2|^2}{1-\cdots}}\ . \tag{29}$$

Equations (27) and (28) are valid for arbitrary pump and probe intensities and all our numerical calculations are based on these exact equations. Our results for a strong pump and moderate probe (see Fig. 2) reveal opposite tendencies for probe and pump absorption when they are considered as a function of the probe frequency ω_2. A qualitative discussion of these effects has been given in the Introduction. This interpretation is based in part on an analysis of the results in the limit of low probe intensity. For weak probes and $\omega_1=\omega_{ba}$, we find to order V_2 and to all orders in $|V_1|^2$ (V_2 is assumed to be real in this calculation)

$${\rm Im}\rho_{ba}(\omega_2)=-AV_2T_2(1+B|V_1|^2T_2^2-C|V_1|^4T_2^4)\ , \tag{30}$$

with

$$A=\frac{(\rho_{bb}-\rho_{aa})^{dc}}{\Delta_2^2T_2^2+1}\ , \tag{31}$$

$$B=[\delta^2T_2^2(3+\delta^2T_2^2)-T_2/T_1]D^{-1}\ , \tag{32}$$

$$C=4(1+\delta^2T_2^2)D^{-1}\ , \tag{33}$$

$$4D=(4\,|\,V_1\,|^2T_2^2+T_2/T_1-\delta^2T_2^2)^2+\delta^2(1+T_2/T_1)^2\ . \tag{34}$$

The first term on the right-hand side of Eq. (30) gives a contribution to the absorbed probe *intensity* of an optically thin sample proportional to $|\,V_2\,|^2$. This term corresponds to a one-probe-photon absorption process.[12] Apart from the one-photon absorption process, the first term necessarily also describes the spontaneous emission of a photon since otherwise the system would not reach the steady state. This spontaneous emission is contained in the A factor [see Eqs. (30) and (31)] and is therefore also present in the two other terms of Eq. (30).

The pump laser does not affect the line shape of the one-photon probe-absorption term but only its intensity via the population inversion factor $(\rho_{bb}-\rho_{aa})^{dc}$ [see Eq. (31)]. Thus the four-level scheme of Fig. 6 (where relaxation effects are omitted), which results from the Rabi splitting of the upper and lower levels of the two-level system interacting with the pump laser, has *no* one-photon probe resonance peaks at $\omega_2=\omega_{ba}\pm2\,|\,V_1\,|$. This shows that the scheme of dressed-atom levels is only meaningful in the actual presence of resonant dressing pump photons and therefore the probe-photon resonance frequencies at $\omega_2=\omega_{ba}\pm2\,|\,V_1\,|$ will only occur in processes involving at least one resonant pump photon. We note, however, that the resonant two-photon processes of Fig. 6 cannot lead to either absorption or stimulated emission because of exact compensation between the processes depicted in Figs. 6(a) and 6(b). Nevertheless, the fact that both processes do occur is clear from the ground-state stabilization produced by them (see Fig. 3).

The second term in Eq. (30), with B given by Eq. (32), gives a contribution proportional to $|\,V_1\,|^2\,|\,V_2\,|^2$ to the absorbed probe *intensity* and describes a two-laser-photon process involving one probe and one pump photon.[12] The third term in Eq. (30) with C given by Eq. (33) gives a contribution proportional to $|\,V_1\,|^4\,|\,V_2\,|^2$ to stimulated probe emission and corresponds to a three-laser-photon process involving one probe photon and two pump photons.[12] The competition between the second and third terms is responsible for the dispersive behavior in the case of saturating pump intensity when

$$|\,V_1\,|^2\gg T_2^{-2}\ , \tag{35}$$

since it follows from Eqs. (30), (32), (33), and (35) that when

$$|\,\Delta_2\,|>2\,|\,V_1\,| \tag{36}$$

there is probe absorption and when

$$|\,\Delta_2\,|<2\,|\,V_1\,| \tag{37}$$

there is stimulated probe emission. As discussed above, the presence of the factor A in Eq. (30) implies that the two- and three-laser photon processes are both accompanied by the spontaneous emission of a scattered photon and may therefore be assumed to correspond to a three-photon (TPS) and a four-photon scattering (FPS) process, respectively (see Figs. 7–10).[13]

In the stimulated emission region, defined by Eq. (37),

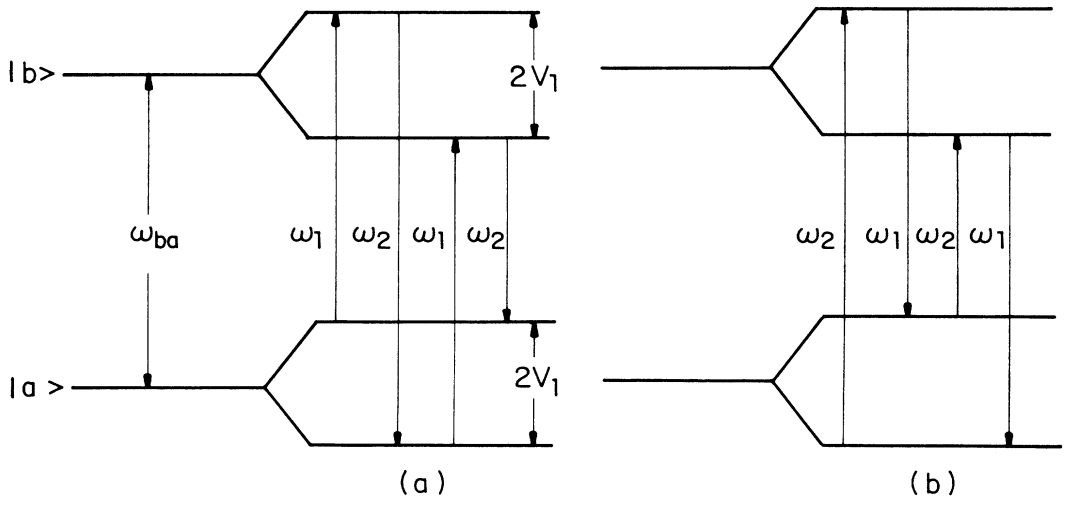

FIG. 6. Two-laser-photon process leading to relative ground-state stabilization. The two-level system interacts resonantly with the strong pump laser: $\Delta_1=\omega_{ba}-\omega_1=0$. The probe laser is at one of the Rabi sideband frequencies: $|\,\Delta_2\,|\equiv|\,\omega_{ba}-\omega_2\,|=2\,|\,V_1\,|$. There is no reason to prefer pump absorption followed by stimulated probe emission, as in (a), over the reverse process of (b). This explains the lack of net absorption or stimulated emission due to these two opposing two-photon processes at the center of the dispersive absorption profile. However, the two processes produce relative ground-state stabilization, which explains the population dips of Fig. 3.

the higher-order nonlinear term of Eqs. (30) and (32), which involves an additional *pump* photon, becomes more important than the lower-order ones and may even prevail over the linear term of Eqs. (30) and (31), leading to overall probe gain as depicted in Fig. 1. As discussed below, we believe that the higher-order nonlinear process prevails here over the lower-order ones because it acquires an almost resonant character when $|\Delta_2|<2|V_1|$ in contrast to the nonresonant character of the lower-order processes. At $\Delta_2=0$, these processes also become resonant and probe gain disappears. Probe gain also disappears outside the power-broadening region where $|\Delta_2|>2|V_1|$ because then the FPS process loses its almost resonant character. The centers of the dispersive features of the probe-absorption spectrum are situated at the dressed-atom state resonances

$$\delta=\Delta_2\simeq\pm 2|V_1| \tag{38}$$

determined by the resonance denominator D of Eq. (34). The second and third terms of Eq. (30) give rise to a narrow homogeneous burning dip in the probe absorption spectrum at resonance in a collisional environment:

$$1/T_2>1/T_1 \tag{39}$$

provided that

$$4|V_1|^2<1/T_2^2 . \tag{40}$$

This effect has been discussed extensively by Boyd and Mukamel.[14]

In the presence of an intense pump laser one would expect that the absorption of the probe laser should decrease due to saturation. The dispersive behavior, where at probe frequencies given by Eq. (39) the probe absorption may be larger than that obtained in the absence of pump absorption, is surprising. Equally surprising is the fact that amplification may occur at frequencies given by the inequality of Eq. (37). It follows from the discussion of Eq. (30) that these effects arise from multiphoton processes (TPS and FPS). For a qualitative understanding of the relative influence of these processes on the dispersive line shape, we again assume that

$$V_1\gg(1/T_1),(1/T_2) , \tag{41}$$

so that the centers of the dispersive feature are determined by Eq. (38).

Then, we note that the interaction of the two-level system with the resonant pump laser produces the Stark-split-level scheme of Figs. 6—11.[12,13] For probe frequencies given by the "resonance" frequency $|\Delta_2|=2|V_1|$ there is no reason to prefer probe emission following pump absorption as shown in Fig. 6(a) over the reverse process, shown in Fig. 6(b).[15] However, when the probe frequency is in the range $|\Delta_2|<2|V_1|$ [see Eq. (37)] and the pump laser is at resonance, the schemes illustrated in Fig. 7 may be invoked. These schemes describe FPS processes. The virtual states $|\alpha\rangle$ and $|\beta\rangle$ are within the power-broadening width of the *pump* laser which *connects* them and therefore the FPS processes are almost resonant in this case. For this reason, the schemes of Fig. 7 prevail over the competing schemes of Fig. 8 which depict TPS in a nonresonant process because the virtual state $|\alpha\rangle$ ($|\beta\rangle$) is *not connected* to the upper state $|b\rangle$ (lower state $|a\rangle$) by the strong *pump* laser, as in Fig. 7. Thus although virtual states $|\alpha\rangle$ and $|\beta\rangle$ are again within the power-broadening width of the *pump* laser, this process is not an almost resonant process since the pump power-broadening width is only meaningful for transitions caused by the pump laser itself.

When the probe frequency is in the range $|\Delta_2|<2|V_1|$, the TPS process of Fig. 10 dominates the FPS of Fig. 9. The reason for this is that now the virtual states of $|\alpha\rangle$ and $|\beta\rangle$ of Fig. 9 are no longer in the power-broadening region of the pump laser so that the FPS process is nonresonant and the lower-order nonlinear TPS process which involves only one virtual state dom-

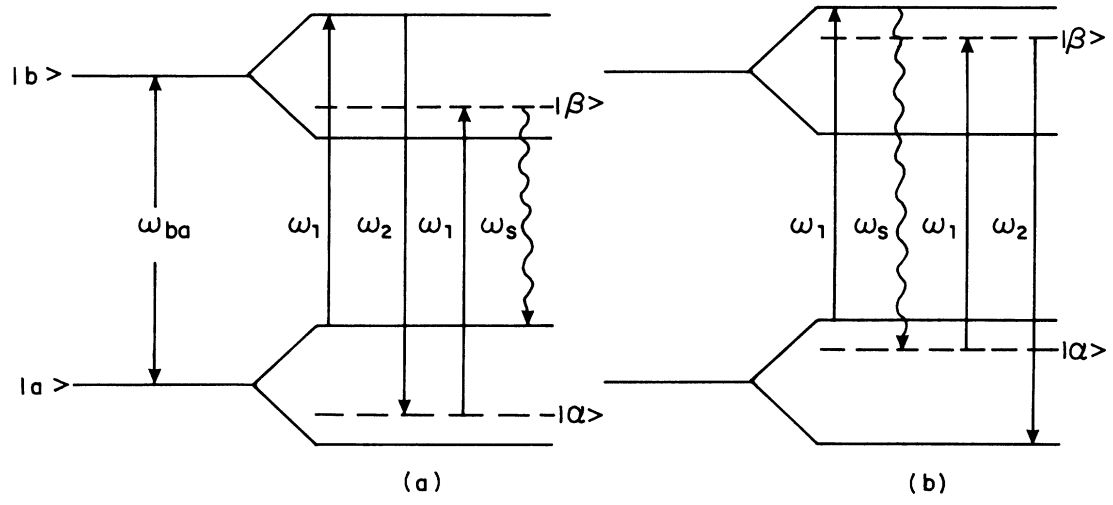

FIG. 7. Irreversible three-laser-photon (or four-photon scattering) process leading to probe amplification, when $\omega_1=\omega_{ba}$ and $|\Delta_2|<2|V_1|$. It dominates the two-laser-photon (or three-photon scattering) process of Fig. 8.

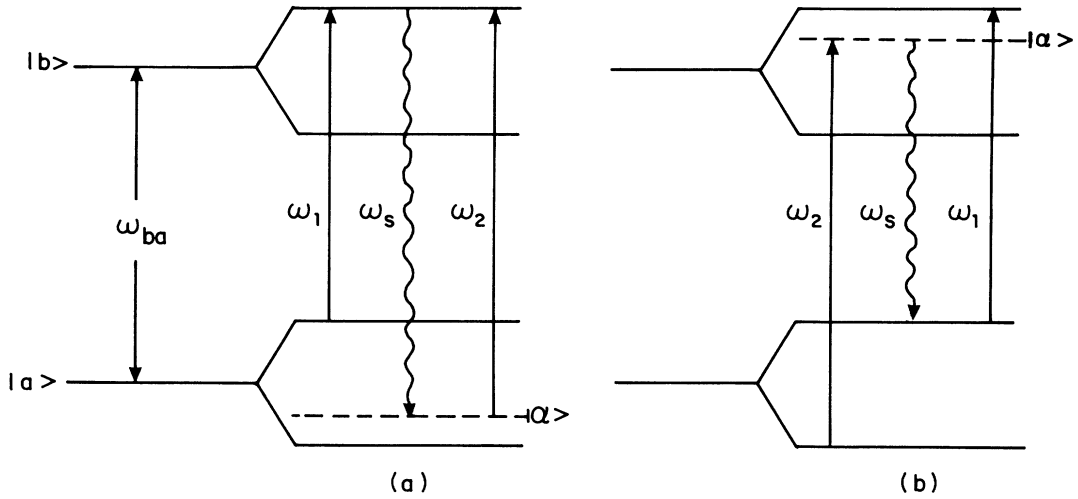

FIG. 8. Irreversible two-laser-photon (or three-photon scattering) process leading to probe absorption, that competes with and is dominated by the process of Fig. 7 when $\omega_1=\omega_{ba}$ and $|\Delta_2|<2|V_1|$.

inates the higher-order nonlinear FPS process which involves two virtual states. It should be stressed that the amplification obtained in the range $|\Delta_2|=|\omega_2-\omega_1|<2|V_1|$ does *not* result from a population difference effect but from the irreversible nature of the (four-photon) scattering process.

As a final point in the discussion of the intuitive meaning of the various terms of Eq. (30), it is worthwhile noting that the detuning appearing in the factors B and C may be considered in two different ways: first, as the detuning of the *probe* frequency with respect to the Rabi-split-level scheme induced by the *pump* laser, and second, as the detuning of the *pump* frequency from the frequency ω_2, interpreted as the transition frequency of the dressed-atom states introduced by the *probe* laser. In the second case, the transition induced by the probe is power broadened by the pump laser. This interpretation may improve the understanding of the difference between Figs. 7 and 9. In Fig. 9, the detuning δ of the second pump-laser photon with respect to ω_2 is larger than the power-broadening width $2|V_1|$, whereas in Fig. 7, it is smaller, thus giving nearly resonant character to the FPS process in this case.

The interpretation of the dispersive probe-absorption spectrum presented here readily leads to, and is corroborated by, the description of the corresponding dispersive absorption spectrum of the pump laser as a function of the probe frequency. This description has already been presented in the Introduction and is not repeated here.

Finally, in Fig. 11 we show the three-photon processes

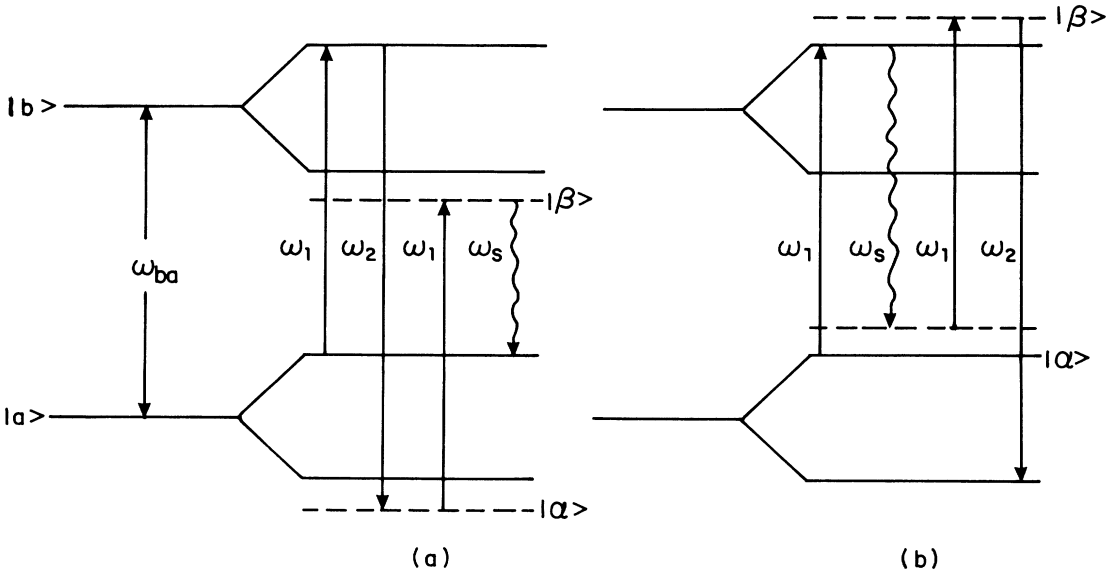

FIG. 9. Irreversible four-photon scattering process for probe amplification when $\omega_1=\omega_{ba}$ and $|\Delta_2|>2|V_1|$. It is identical to the process described in Fig. 7, but in this range of probe frequencies, it is dominated by the three-photon scattering process of Fig. 10.

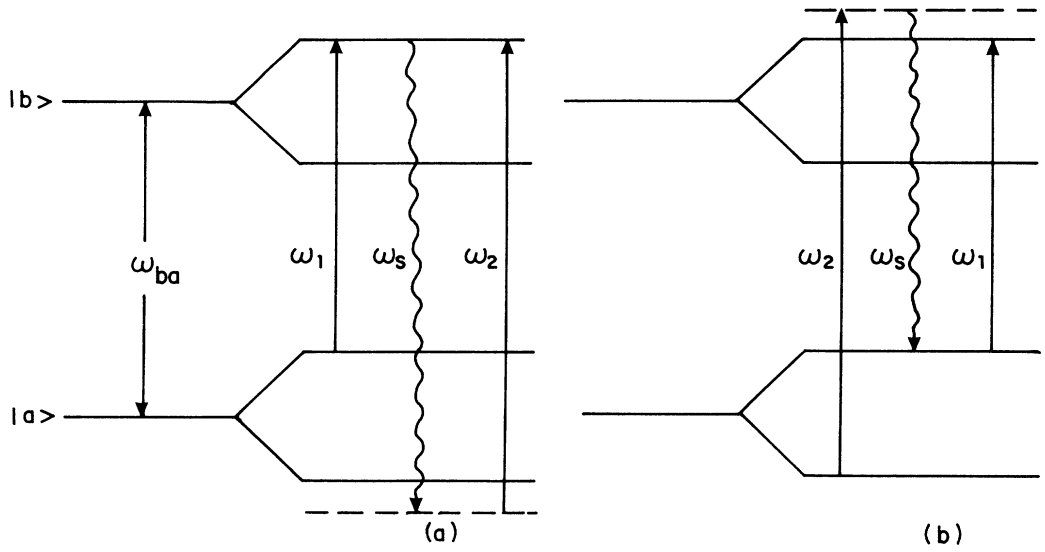

FIG. 10. Irreversible three-photon scattering process leading to probe absorption that dominates the four-photon scattering process of Fig. 9 when $\omega_1=\omega_{ba}$ and $|\Delta_2|>2|V_1|$.

responsible for the two Rabi subharmonic peaks in the distorted dispersion profile of the probe absorption spectrum for the case of a strong pump and a moderately strong probe and the corresponding dips in the pump absorption spectrum [see Fig. 2(a)].

Figures 7—10 provide a qualitative understanding of the quantitative results obtained in this paper. In these figures abundant use is made of states dressed with photons of two frequencies whereas the quantitative theoretical results were derived using bare-atom states. It would therefore seem appropriate to reformulate the problem in terms of states dressed with photons of two frequencies. However, due to the complexity of the interaction of a relaxing two-level system with two intense fields, the theoretical effort may well be prohibitive.

Furthermore, it would be interesting to obtain experimental confirmation of the theory showing that, at moderate probe intensity, part of the scattered photon spectrum is closely connected to the probe absorption spectrum since there is a one-to-one correspondence between the absorbed (emitted) probe photons in TPS (FPS) and the scattered photons.

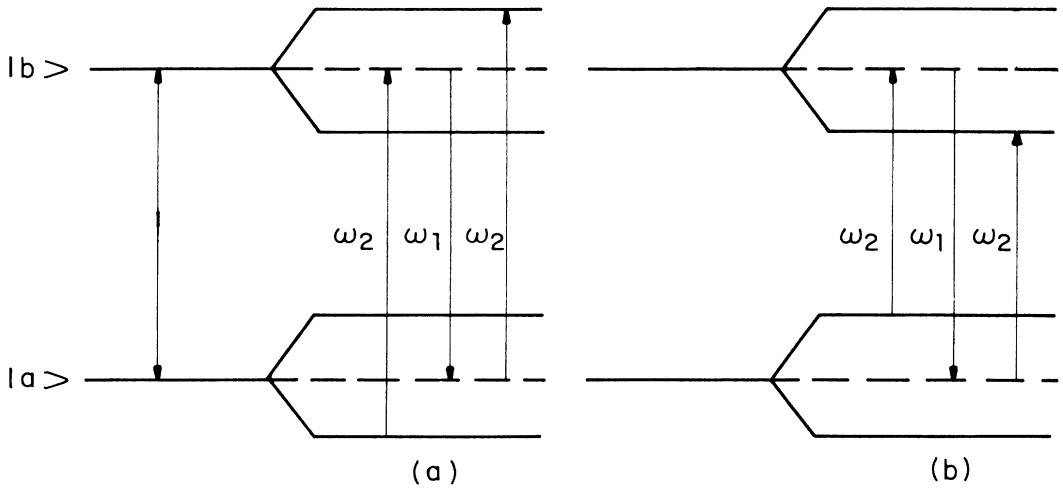

FIG. 11. Three-photon processes producing Rabi subharmonic peaks in the probe-absorption spectrum and corresponding dips in the pump-absorption spectrum. Clearly, these peaks lie at the probe frequencies $\omega_2=\omega_1+|V_1|$, which corresponds to a probe detuning, $\omega_2-\omega_1$, which is one-half that of the Rabi sideband frequencies. The peaks in the probe absorption arise because in the three-photon process, two probe-laser photons are absorbed and the corresponding dips in the pump absorption spectra are due to the emission of a pump photon in the three-photon process.

[1]B. R. Mollow, Phys. Rev. **188**, 1969 (1969).
[2]F. Schuda, C. R. Stroud, Jr., and M. Hercher, J. Phys. B **7**, L198 (1974).
[3]J. L. Carlsten, A. Szoke, and M. G. Raymer, Phys. Rev. A **15**, 1029 (1977).
[4]B. R. Mollow, Phys. Rev. A **5**, 2217 (1972).
[5]F. Y. Wu, S. Ezekiel, M. Ducloy, and B. R. Mollow, Phys. Rev. Lett. **38**, 1077 (1977).
[6]G. I. Toptygina and E. E. Fradkin, Zh. Eksp. Teor. Fiz. **82**, 429 (1982) [Sov. Phys.—JETP **55**, 246 (1982)].
[7]G. S. Agarwal and N. Nayak, J. Opt. Soc. Am. B **1**, 264 (1984); Phys. Rev. A **33**, 391 (1986).
[8]A. M. Bonch-Bruevich, S. G. Przhibel'skii, and N. A. Chigir', Zh. Eksp. Teor. Fiz. **80**, 565 (1981) [Sov. Phys.—JETP **53**, 285 (1981)]; A. M. Bonch-Bruevich, T. A. Vartanyan, and N. A. Chigir', *ibid.* **77**, 1899 (1979) [*ibid.* **50**, 901 (1979)].
[9]R. Guccione-Gush and H. P. Gush, Phys. Rev. A **10**, 1474 (1974).
[10]N. Tsukuda, J. Phys. Soc. Jpn. **46**, 1280 (1979).
[11]R. W. Boyd, M. G. Raymer, P. Narum, and D. J. Harter, Phys. Rev. A **24**, 411 (1981).
[12]Because of the saturation implicit in the population inversion factor $(\rho_{bb}-\rho_{aa})^{dc}$ [see Eq. (31)] and in the denominator D [see Eq. (34)], all numbers of ω_1 photons will contribute. However, the physical meaning of the various terms of Eq. (30) is obtained by omitting the saturation denominators and considering only the numerators which survive in the perturbation limit and describe all possible multiphoton processes in the two-level system in the steady state and in the perturbation limit, provided only one probe photon and one scattered photon are involved. The schematic description of multiphoton processes under saturation conditions using only a minimal number of pump photons is quite common in the literature (see, for example, Ref. 15 and the references therein). In these schemes, the strong interaction with the pump is taken into account by using dressed-atom (or Rabi-split) states and the multiphoton processes which involve the probe and/or the scattered photon are treated by perturbation theory. A theoretical justification for this procedure is given by P. Verkerk, M. Pinard, and G. Grynberg, Phys. Rev. A **34**, 4008 (1986).
[13]In the schemes appearing in Figs. 7–10, only the case where $\omega_2>\omega_1$ is considered. There are eight analogous diagrams for $\omega_2<\omega_1$.
[14]R. W. Boyd and S. Mukamel, Phys. Rev. A **29**, 1973 (1984).
[15]It is interesting to note that when the probe photon is replaced by a scattered photon, the process becomes irreversible and a peak appears in the scattered spectrum at $|\Delta_2|=2|V_1|$ (see Ref. 1).